Modeling CO_2 exchange over a Bornean tropical rain forest using measured vertical and horizontal variations in leaf-level physiological parameters and leaf area densities

Tomo`omi Kumagai,[1] Tomoaki Ichie,[2] Mitsunori Yoshimura,[3] Megumi Yamashita,[4] Tanaka Kenzo,[5] Taku M. Saitoh,[6] Mizue Ohashi,[7] Masakazu Suzuki,[8] Takayoshi Koike,[9] and Hikaru Komatsu[10]

Received 16 September 2005; revised 16 January 2006; accepted 22 February 2006; published 31 May 2006.

[1] Southeast Asian tropical rain forests are among the world's most important biomes in terms of global carbon cycling; nevertheless, the impact of environmental factors on the ecosystem CO_2 flux remains poorly understood. One-dimensional multilayer biosphere-atmosphere models such as soil-vegetation-atmosphere transfer (SVAT) models are promising tools for understanding how interactions between environmental factors and leaf-level physiological parameters might impact canopy-level CO_2 exchange. To examine application of the SVAT model in tropical rain forests, which is expected to be difficult partly because of the complex canopy structure and large number of tree species, we measured vertical and horizontal variations in leaf-level physiological parameters and leaf area densities together with eddy covariance measurements using a canopy crane in a tropical rain forest in Sarawak, Malaysia. Despite differences in species and canopy positions, leaf nitrogen per unit area (N_a) within the canopy could be one-dimensionally described as a linear function of height. N_a also clearly explained the other leaf-level physiological parameters across species and canopy positions. Even though the leaf area density profile likely varies in this tropical forest, the SVAT model satisfactorily reproduced the eddy covariance measurements. Furthermore, the CO_2 flux calculated on the assumption that N_a measured in the upper canopy was distributed evenly throughout was almost the same as that taking the vertical gradient into consideration. These findings suggest that when reproducing the CO_2 flux in tropical rain forests using the SVAT model, the leaf area density profile obtained from the leaf area index (LAI) measured at one point and leaf-level physiological properties measured across species in the upper canopy are sufficient.

Citation: Kumagai, T., T. Ichie, M. Yoshimura, M. Yamashita, T. Kenzo, T. M. Saitoh, M. Ohashi, M. Suzuki, T. Koike, and H. Komatsu (2006), Modeling CO_2 exchange over a Bornean tropical rain forest using measured vertical and horizontal variations in leaf-level physiological parameters and leaf area densities, *J. Geophys. Res.*, *111*, D10107, doi:10.1029/2005JD006676.

1. Introduction

[2] Tropical rain forests cover about 12% of the total land surface, possibly containing up to 55% of the carbon in the terrestrial biosphere [*Whittaker and Likens*, 1975; *Grace et al.*, 2001]. These forests are also highly productive and responsible for about 50% of the total terrestrial net primary productivity [*Grace et al.*, 2001]. Therefore a small perturbation in this biome could result in a significant change in the global carbon cycle [*Taylor and Lloyd*, 1992].

[3] Although tropical forests in Southeast Asia represent about 17% of the total tropical rain forest area [*Food and Agriculture Organization*, 1993], relative deforestation rates [*Malhi and Grace*, 2000] and estimated resulting CO_2 emissions [*Houghton and Hackler*, 1999; *Malhi and Grace*, 2000] are the highest in the region. These forests remain a viable resource for the economies of several Southeast Asian countries such as Malaysia, yet their potential as a carbon sink has received much less attention than that of Amazonian rain forests [*Fan et al.*, 1990; *Grace et al.*, 1995; *Lloyd et al.*, 1995; *Grace et al.*, 1996; *Malhi et al.*, 1998; *Williams et al.*, 1998; *Vourlitis et al.*, 2001; *Saleska et al.*, 2003]. What is also less certain is an understanding of how potential shifts in land use and environmental factors

[1] Shiiba Research Forest, Kyushu University, Shiiba-son, Miyazaki, Japan.
[2] Faculty of Agriculture, Kochi University, Nankoku, Japan.
[3] Research Institute for Humanity and Nature, Kyoto, Japan.
[4] Survey College of Kinki, Osaka, Japan.
[5] Forestry and Forest Products Research Institute, Tsukuba, Japan.
[6] River Basin Research Center, Gifu University, Gifu, Japan.
[7] Joensuu Research Center, Finnish Forest Research Institute, Joensuu, Finland.
[8] Graduate School of Agricultural and Life Sciences, University of Tokyo, Tokyo, Japan.
[9] Hokkaido University Forests, FSC, Sapporo, Japan.
[10] Institute of Industrial Science, University of Tokyo, Tokyo, Japan.

0148-0227/06/2005JD006676$09.00

might impact the biosphere-atmosphere CO_2 exchange from these tropical rain forests.

[4] To describe the CO_2 flux from forested ecosystems, a number of one-dimensional multilayer biosphere-atmosphere models such as soil-vegetation-atmosphere transfer (SVAT) models have been developed, coupling ecophysiological and biogeochemical principles at the leaf scale with detailed turbulent transport mechanics [*Baldocchi*, 1992; *Baldocchi and Meyers*, 1998; *Lai et al.*, 2000a, 2000b, 2002; *Baldocchi and Wilson*, 2001; *Siqueira et al.*, 2002; *Tanaka*, 2002; *Park and Hattori*, 2004; *Watanabe et al.*, 2004]. Practically, the model based on the SVAT framework has been shown to clearly reproduce measured scalar fluxes in several vegetation types [e.g., *Baldocchi and Meyers*, 1998] and on hourly to multiyear timescales [e.g., *Baldocchi and Wilson*, 2001]. Furthermore, using a model that coupled the SVAT approach with a plant size distribution model, *Watanabe et al.* [2004] were able to describe the dynamics of a forest ecosystem; for example, in terms of competition, growth and mortality of trees. Once the SVAT model has been validated against measurements taken in a given forested ecosystem, it can be used to enhance our understanding of how interactions between microclimates and leaf-level physiological parameters might impact canopy-level gas exchange, and consequently, forest dynamics.

[5] Tropical rain forests are characterized by their great stature and complex canopy structure, wide range of life forms, and large number of tree species [*Koike and Syahbuddin*, 1993; *Grace et al.*, 2001], all of which result in strong vertical gradients of environmental [*Cabral et al.*, 1996; *Kumagai et al.*, 2001] and physiological factors [*Roberts et al.*, 1990, 1993; *Dolman et al.*, 1991; *McWilliam et al.*, 1996; *Carswell et al.*, 2000]. There is also considerable horizontal heterogeneity in tropical rain forests [*Grace et al.*, 2001]. In the SVAT model, however, canopy structure is described by an area-averaged representation, with even the one-dimensional vertical variation in physiological properties being considered in only a few studies [*Lai et al.*, 2002; *Watanabe et al.*, 2004]. Application of the SVAT model in tropical rain forests therefore needs to account for two major sources of error: spatial variations in leaf-level physiological parameters such as photosynthetic capacity and regulation of stomatal conductance, and leaf area densities.

[6] In this study, we examine how large the spatial variations in leaf-level physiological parameters and leaf area densities are in a tropical rain forest and whether the SVAT model can be applied to tropical rain forests by comparing model results with measurements collected as part of a previous project [*Nakashizuka et al.*, 2001]. A canopy crane installed in a Southeast Asian tropical rain forest [see *Ozanne et al.*, 2003, Figure 1] allowed canopy access and freedom to take spatially detailed measurements of the physiological status and structure of the canopy. Using these measurements, a multilayer ecophysiological and turbulent transport model was used to simulate CO_2 exchange over the canopy. We emphasize that our model was parameterized by independently collected ecophysiological measurements, and was not calibrated or parameterized by canopy-level flux measurements. Also, the outputs from the model were independently validated using eddy covariance flux measured at the top of the canopy. After validation, a SVAT model can be used to examine how detailed model input measurements must be and how far the model can be simplified while reasonably reproducing the flux measurements. Therefore the SVAT model can serve a tool to provide strategies for measuring and modeling CO_2 fluxes in tropical rain forests.

2. Theory

[7] Our SVAT model consists of three submodels: (1) a model for energy and radiation conservation, (2) an ecophysiological model for stomatal opening and carbon assimilation, and (3) a model for turbulent diffusion. In all computations, the canopy is divided into layers, each of thickness Δz (m), and all equations detailed below are solved at each layer.

2.1. Radiative Transfer and Energy Balance of Leaves and the Soil Surface

[8] Radiative transfer within the canopy was modeled using the modified *Tanaka* [2002] formulation. Radiation incident on the canopy is decomposed into solar and thermal radiation. When determining the penetration of solar radiation through the canopy, we must separately consider direct beam and diffuse irradiance due to their different attenuation in the canopy. Both direct and diffuse solar radiation can be further divided into photosynthetically active radiation (PAR) and near-infrared radiation (NIR) according to their different absorption by leaves [e.g., *Goudriaan*, 1977; *Ishida et al.*, 2001]. Note that approximately half the solar radiation over the canopy is in the form of PAR while the other half is in the form of NIR wave bands [e.g., *Campbell and Norman*, 1998]. Thus appropriate parameters for scattering, reflection and extinction within the canopy must be used for each wave band, and the irradiance absorption and energy balance need to be computed separately for sunlit and shaded leaves [e.g., *Wang and Jarvis*, 1990; *Leuning et al.*, 1995; *de Pury and Farquhar*, 1997].

[9] The absorbed PAR or NIR within a canopy layer between z (the height from the ground, m) and $z + \Delta z$, ΔS (W m^{-2}), is defined as:

$$\Delta S_b = (1 - \eta - \xi)(1 - P_b)S_b(z + \Delta z) \quad (1)$$

$$\Delta S_d^{\downarrow} = (1 - \eta - \xi)(1 - P_d)S_d^{\downarrow}(z + \Delta z) \quad (2)$$

$$\Delta S_d^{\uparrow} = (1 - \eta - \xi)(1 - P_d)S_d^{\uparrow}(z) \quad (3)$$

where η and ξ are the leaf transmissivity and reflectivity, respectively, for PAR or NIR, P is the probability of no contact with the irradiance within that canopy layer, and S is PAR or NIR at the given height (W m^{-2}). Subscripts b and d denote direct beam and diffuse irradiation, respectively, and superscript arrows denote the direction of the irradiation. The total absorbed solar radiation within that canopy layer, ΔS^t (W m^{-2}), is then calculated as the sum of the absorbed PAR and NIR, both of which are calculated by (1)–(3). The total solar radiation absorbed by sunlit

Table 1. Parameters Used for Modeling Radiative Transfer and Energy Balance

Variable	Value	Reference
Leaf transmissivity for PAR and NIR, η	0.03 and 0.25	*Ishida et al.* [2001]
Leaf reflectivity for PAR and NIR, ξ	0.1 and 0.4	*Ishida et al.* [2001]
Soil reflectivity for PAR and NIR, ξ_s	0.06 and 0.38	*Campbell and Norman* [1998]
Leaf emissivity, ε_l	0.98	*Campbell and Norman* [1998]
Soil emissivity, ε_s	0.95	*Campbell and Norman* [1998]

(S^t_{absl}: W m^{-2}) and shaded leaves (S^t_{absh}: W m^{-2}) is expressed as:

$$S^t_{absl} = \Delta S^t_b + \frac{a_{sl}}{a_{leaf}}\left(\Delta S^{t\downarrow}_d + \Delta S^{t\uparrow}_d\right) \tag{4}$$

$$S^t_{absh} = \frac{a_{sh}}{a_{leaf}}\left(\Delta S^{t\downarrow}_d + \Delta S^{t\uparrow}_d\right) \tag{5}$$

where a_{leaf}, a_{sl} and a_{sh} are the total, sunlit and shaded leaf area densities (m^2 m^{-3}) within a given layer, respectively. The total solar radiation absorbed by the soil surface (S^t_{absoil}: W m^{-2}) is given by:

$$S^t_{absoil} = \left(1-\xi^P_s\right)\left[S^P_b(0) + S^{P\downarrow}_d(0)\right] + \left(1-\xi^N_s\right)\left[S^N_b(0) + S^{N\downarrow}_d(0)\right] \tag{6}$$

where ξ_s is the soil reflectivity, and the superscripts P and N indicate PAR and NIR, respectively. The PAR absorbed by sunlit (Q_{absl}: μmol m^{-2} s^{-1}) and shaded leaves (Q_{absh}: μmol m^{-2} s^{-1}) is given by:

$$Q_{absl} = \omega\left(\frac{\Delta S^P_b}{a_{sl}\Delta z} + \frac{\Delta S^{P\downarrow}_d + \Delta S^{P\uparrow}_d}{a_{leaf}\Delta z}\right) \tag{7}$$

$$Q_{absh} = \omega\frac{\Delta S^{P\downarrow}_d + \Delta S^{P\uparrow}_d}{a_{leaf}\Delta z} \tag{8}$$

where ω is the unit conversion factor (4.6 μmol J^{-1}) [*Campbell and Norman*, 1998]. Note that S^t_{absl} and S^t_{absh} are expressed per unit area of ground, whereas Q_{absl} and Q_{absh} are expressed per unit of leaf area.

[10] The absorbed thermal radiation within a canopy layer between z and $z + \Delta z$, L_{ab} (W m^{-2}), is defined as:

$$L_{ab} = (1-P_d)L^{\uparrow}(z) + (1-P_d)L^{\downarrow}(z+\Delta z) \tag{9}$$

where L is the thermal radiation at the given height (W m^{-2}). L_{ab} within canopy layers of sunlit (L_{absl}: W m^{-2}) and shaded leaves (L_{absh}: W m^{-2}) is calculated by multiplying L_{ab} by a_{sl}/a_{leaf} and a_{sh}/a_{leaf}, respectively.

[11] Assuming that soil heat storage can be neglected, the energy balance equation is given by:

$$S^t_{absoil} + L^{\downarrow}(0) - \varepsilon_s\sigma T^4_g = \lambda\rho_a\Omega g_{Hs}\left[q_{sat}\left(T_g\right) - q\left(z_g+\Delta z\right)\right] + \rho_a c_p g_{Hs}\left[T_g - T\left(z_g+\Delta z\right)\right] \tag{10}$$

where ε_s is the soil emissivity, σ is the Stefan-Boltzmann constant (5.67 × 10^{-8} W m^{-2} K^{-4}), T_g is the soil surface temperature (K), λ is the latent heat of vaporization of water (J kg^{-1}), ρ_a is the density of air (kg m^{-3}), Ω is the soil surface moisture availability, q is the specific humidity of air (kg kg^{-1}) at a given height, $q_{sat}(T_g)$ is the saturation value (kg kg^{-1}) at T_g, z_g is roughness length of the soil surface (m), c_p is the specific heat of air at constant pressure (J kg^{-1} K^{-1}), and T is the air temperature (K) at a given height. Using the logarithmic wind law, we assume that the heat conductance at the soil surface (g_{Hs}: m s^{-1}) is given by $\kappa\, u(z_g+\Delta z)^2/\{\ln[(z_g+\Delta z)/z_g]\}^2$, where κ is von Karman's constant (0.4) and u is the wind velocity (m s^{-1}) at a given height. The energy balance on sunlit and shaded leaf surfaces within a canopy layer between z and $z + \Delta z$ is expressed by:

$$S^t_{absl} + L_{absl} - 2(1-P_d)\varepsilon_l\sigma T^4_{csl}a_{sl}/a_{leaf} = \lambda E_{lsl}a_{sl}\Delta z + H_{lsl}a_{sl}\Delta z \tag{11}$$

$$S^t_{absh} + L_{absh} - 2(1-P_d)\varepsilon_l\sigma T^4_{csh}a_{sh}/a_{leaf} = \lambda E_{lsh}a_{sh}\Delta z + H_{lsh}a_{sh}\Delta z \tag{12}$$

where ε_l is the leaf emissivity, T_c is the leaf temperature (K), and the subscripts *sl* and *sh* denote sunlit and shaded leaves, respectively. E_l and H_l represent, respectively, the water vapor (kg m^{-2} s^{-1}) and sensible heat fluxes (W m^{-2}) expressed per unit of leaf area; these are described in the next section.

[12] Parameters representing the radiative properties of a leaf and soil are listed in Table 1. The details of the formulation and parameterization of P_b, P_d, S_b, S_d, a_{sl}, a_{sh}, and L related to solar geometry, light and the canopy structure are described in Appendix A.

2.2. Leaf-Level Physiological Functions

[13] Assuming hypostomatous leaves, the leaf-level scalar source strengths, i.e., H_l, E_l, and the leaf photosynthesis rate (A_l; μmol m^{-2}s^{-1}) are derived from physiological controls using:

$$H_l = 2m_a c_p g_{ah}(T_c - T) \tag{13}$$

$$E_l = m_e\frac{g_{aw}g_{sw}}{g_{aw}+g_{sw}}\frac{[e_{sat}(T_c) - e]}{P} \tag{14}$$

$$A_l = g_{ac}(C_a - C_s) \tag{15}$$

$$= g_{sc}(C_s - C_i) \tag{16}$$

where m_a and m_e are the molecular weights of air and water (kg mol^{-1}), respectively; $e_{sat}(T_c)$ and e are the saturation vapor pressure at T_c and atmospheric water vapor pressure (Pa), respectively; P is the atmospheric pressure (Pa); and C_s, C_a and C_i are the CO_2 concentrations (μmol mol^{-1}) of air inside and outside the laminar boundary layer of leaves and within the stomatal cavity, respectively.

[14] g_{ah}, g_{aw} and g_{ac} are the boundary layer conductances for heat, water vapor and CO_2 (mol m^{-2} s^{-1}), respectively. Determination of the contribution of buoyancy forces on boundary layer conductances of sunlit leaves deep within the canopy where wind speeds are low is important, because without taking this mechanism into account computed leaf temperatures become excessively high [*Leuning et al.*, 1995]. Thus the contribution of both forced and free convection on scalar exchange through leaf boundary layers was considered, giving the total boundary layer conductance for species j, heat, water vapor and CO_2, for one side of a leaf, g_{aj} (mol $m^{-2}s^{-1}$), as:

$$g_{aj} = g_{ajw} + g_{ajf} \tag{17}$$

where g_{ajw} and g_{ajf} are the boundary layer conductances for species j resulting from forced and free convection (mol $m^{-2}s^{-1}$), respectively, calculated according to *Campbell and Norman* [1998].

[15] g_{sw} and g_{sc} are the stomatal conductances for water vapor and CO_2 (mol m^{-2} s^{-1}), respectively. g_{sc} is linked to A_l, the relative humidity of air inside the boundary layer of a leaf (h_s) and C_s, as described by *Ball et al.* [1987] and *Collatz et al.* [1991], and is given by:

$$g_{sc} = m\frac{A_l h_s}{C_s} + b \tag{18}$$

where m and b are, respectively, the slope and intercept obtained by linear regression analysis of data from leaf-level gas exchange measurements. g_{sw} is obtained from g_{sw} = 1.6 g_{sc}, where 1.6 is the ratio of diffusivities of CO_2 and water in air [*von Caemmerer and Farquhar*, 1981].

[16] Leaf photosynthesis was computed using the biochemical models of *Farquhar et al.* [1980] and *Collatz et al.* [1991]:

$$A_l = \min\{J_E, J_C, J_S\} - R_d \tag{19}$$

where J_E, J_C and J_S are the gross rate of photosynthesis (μmol $m^{-2}s^{-1}$) limited by the rate of ribulose bisphosphate (RuBP) regeneration through electron transport, RuBP carboxylase-oxygenase (Rubisco) activity and the export rate of synthesized sucrose, respectively, and R_d is the respiration rate (μmol $m^{-2}s^{-1}$) during the day but in the absence of photorespiration. The formulation and parameterization of J_E, J_C, J_S and R_d as a function of the PAR absorbed by a leaf (μmol m^{-2} s^{-1}), C_i and T_c are described by *Farquhar et al.* [1980], *Farquhar and Wong* [1984], *Collatz et al.* [1991] and *de Pury and Farquhar* [1997]. The photosynthesis model constants used in this study were determined according to *Badger and Collatz* [1977], *Farquhar et al.* [1980], *von Caemmerer et al.* [1994] and *de Pury and Farquhar* [1997]. The maximum carboxylation rate when RuBP is saturated (V_{cmax}: μmol m^{-2} s^{-1}) and the potential rate of whole-chain electron transport (J_{max}: μmol m^{-2} s^{-1}) used in these calculations are expressed as nonlinear functions of temperature using their values at 25°C ($J_{max,25}$ and $V_{cmax,25}$, respectively); the formulations are given by *de Pury and Farquhar* [1997]. In addition, R_d is expressed as a nonlinear function of temperature using R_d at 25°C ($R_{d,25}$), which was assumed to be linearly related to $V_{cmax,25}$ [e.g., *Collatz et al.*, 1991].

[17] Practically, both $J_{max,25}$ and $R_{d,25}$ are related to $V_{cmax,25}$, and hence $V_{cmax,25}$ is the key parameter in the leaf photosynthesis model. Variability in $V_{cmax,25}$ as a result of species or vertical canopy gradients is described well by changes in leaf nitrogen per unit area (N_a; g m^{-2}) [e.g., *Wilson et al.*, 2000]. Thus, in line with *Niinements and Tenhunen* [1997], we assume that variation in $V_{cmax,25}$ can be expressed by a linear relationship:

$$V_{c\max,25} = 6.25 V_{cr} R_F N_a \tag{20}$$

where 6.25 is the ratio of the weight of Rubisco to the weight of nitrogen in Rubisco, V_{cr} is the specific activity of Rubisco (≈20.7μmol g^{-1} s^{-1} at 25°C), and R_F is the apparent fraction of nitrogen allocated to Rubisco. *Wilson et al.* [2000] also showed that temporal changes in $V_{cmax,25}$ are poorly correlated with N_a probably because of seasonally dependent R_F. In their study, variations in R_F as a result of species, the vertical canopy gradient and seasonality were between 0.03 and 0.33.

[18] The leaf photosynthesis model calculates A_l for both sunlit and shaded leaves. The A_l calculated in (19) is coupled with g_{sc} using (18), and hence determination of A_l requires C_s, C_i, h_s and T_c, which result from e, C_a and T using (13)–(16). Thus all three scalar (e, C_a and T) transport equations and (13)–(16) must be simultaneously considered, as described next.

2.3. Scalar Transport

[19] The scalar continuity and turbulent flux equations are obtained by assuming a steady state planar-homogeneous and high Reynolds and Peclet numbers flow, and by applying time and horizontal averaging [e.g., *Yamada*, 1992; *Katul and Albertson*, 1999]. The source (or sink) terms, due to mass release (or uptake) by the ensemble of leaves within the averaging plane, in the scalar continuity equations are given by:

$$S_T = \frac{1}{\rho_a c_p}(H_{lsl}a_{sl} + H_{lsh}a_{sh}) \tag{21}$$

$$S_q = \frac{1}{\rho_a}(E_{lsl}a_{sl} + E_{lsh}a_{sh}) \tag{22}$$

$$S_c = -(A_{lsl}a_{sl} + A_{lsh}a_{sh}) \tag{23}$$

where S_T, S_q and S_c are the source strengths for heat (K s^{-1}), water vapor (kg kg^{-1} s^{-1}) and the CO_2 concentration (μmol m^{-3} s^{-1}), respectively. The turbulent flux equations include unknowns requiring closure approximations; we used the closure approximations for flux transport and pressure-scalar gradient covariance described by *Mellor* [1973], *Yamada* [1992] and *Watanabe* [1993].

[20] To solve the scalar continuity and turbulent flux equations, velocity statistics within the canopy need to be computed. In this study, the second-order closure model formulated by *Wilson and Shaw* [1977] was applied. Using the measured wind profile and logarithmic law, the momen-

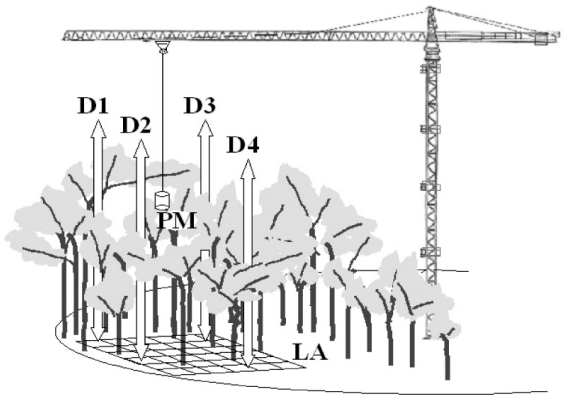

Figure 1. Schematic representation of the canopy crane with adjacent trees. To determine leaf-level physiological parameters, we randomly chose 60 trees and accessed them using the gondola (PM). Subplot LA was used to determine the horizontal variation in the leaf area index (LAI), and the vertical profiles of LAI were measured along four vertical observation lines (D1–D4) using the gondola.

tum roughness length and zero-plane displacement were determined as $0.047h$ and $0.89h$ (where h is the canopy height (m)), respectively. Boundary conditions were specified in accordance with *Katul and Albertson* [1999], and the closure constants given by *Wilson and Shaw* [1977], *Watanabe* [1993] and *Katul and Albertson* [1999] were used. To solve the second-order closure model, we used the numerical scheme described by *Katul and Albertson* [1998, 1999].

3. Study Site and Measurements

[21] While details of the site and instruments relevant to the flux measurements are presented by *Kumagai et al.* [2004a, 2004b], a review and description of the measurements of leaf-level physiological parameters and leaf area densities are provided for completeness.

3.1. Site Description

[22] The experiment was carried out in a natural forest in Lambir Hills National Park (4°12′N, 114°02′E), 30 km south of Miri City, Sarawak, Malaysia. The mean annual rainfall at Miri Airport, 20 km from the study site, for the period 1968–2001 was around 2740 mm with some seasonal variation [e.g., *Kumagai et al.*, 2004a]. The mean annual temperature was around 27°C with little seasonal variation [e.g., *Kumagai et al.*, 2005]. The rain forest in this park consists of two types of original vegetation common to Borneo, mixed dipterocarp and tropical heath forest [*Yamakura et al.*, 1995]. The former contains various types of dipterocarp trees, which cover 85% of the total park area.

3.2. Crane Facility

[23] A 4 ha experimental plot at an altitude of 200 m and on a gentle slope (<5°), gridded into 400 subplots or quadrats of 10×10 m^2, was used in this project. An 80 m tall (at the base of the gondola) canopy crane with a 75 m long rotating jib was constructed in the center of this plot to provide access to the crowns of the study trees (Figure 1). The gondola could be maneuvered both horizontally and vertically with precision. Observational stages at 4 levels (23.5, 38.5, 59.0, and 75.5 m above the ground) accessible by an elevator were also installed. One stage (59.0 m high) was devoted solely to eddy covariance flux measurements. The subplots or quadrats were used for in-canopy micrometeorological measurements. The canopy surrounding the crane is about 40 m high, but the height of emergent treetops can reach up to 50 m.

3.3. Meteorological Measurements

[24] The following instruments were installed at the top of the crane, 85.8 m from the forest floor: a solar radiometer (MS401, EKO, Tokyo, Japan), infrared radiometer (Model PIR, Epply, Newport, Rhode Island), and tipping bucket rain gauge (RS102, Ogasawara Keiki, Tokyo, Japan). The diffuse solar radiation was calculated using the global solar radiation, R_S (Wm^{-2}), and time, t_h (hours) as $-0.00212R_S^2 + 1.21R_S$ ($t_h \leq 9$), $-0.00122R_S^2 + 1.31R_S$ ($9 < t_h \leq 15$) and $4.18R_S^{0.57}$ ($15 < t_h$), which were determined using intensive observation data with the diffuse solar radiometer. At a separate tower located approximately 100 m south of the crane, the upward short-wave and long-wave radiation were measured using a solar radiometer (CM06E, Kipp & Zonen, Delft, Netherlands) and infrared radiometer (Model PIR, Epply, Newport, Rhode Island) installed upside down. These measurements were used to compute net radiation.

[25] At the subplot for the in-canopy microclimate measurements, we sampled mean air temperature and humidity at heights of 41.5, 31.5, 21.5, 11.5, 6.5 and 1.5 m using a series of ventilated sensors with dataloggers (H0803208 and RS1, Onset, Pocasset, Massachusetts) at 10-min intervals. Volumetric soil moisture content, matric potential, soil temperature and soil heat flux were also measured in the subplot using TDR (CS615, Campbell Scientific, Logan, Utah) and tensiometers (DIK3150, Daiki, Tokyo, Japan) at 10, 20 and 50 cm below the forest floor, thermocouples at 2, 10, 20 and 50 cm below the forest floor and a heat flowmeter (MF-81, EKO, Tokyo, Japan) at 10 cm below the forest floor, respectively, at 10-min intervals (CR23X datalogger, Campbell Scientific, Logan, Utah). The soil moisture measurements confirmed that the experimental period (4–20 September 2002) was under well watered condition. The soil heat flux ranged between −3 and 2 W m^{-2} [*Sato et al.*, 2004], and so we assumed that the soil heat storage term in (10) could be neglected.

3.4. Leaf-Level Physiological Measurements

[26] Descriptions of the leaf-level measurements conducted in September 2002 (day of year (DOY) 256–269) are presented by *Kenzo et al.* [2004] and repeated here for completeness. To determine the leaf-level physiological parameters in this site, we randomly chose 60 trees comprising five dipterocarp species that dominate the canopy of tropical rain forests in Southeast Asia (Table 2), and accessed them using the gondola (Figure 1). Gas exchange measurements were obtained for three leaves from each tree using a portable IRGA (LI-6400, Li-Cor, Lincoln, Nebraska) between 0800 and 1100 LT to avoid the midday depression in photosynthesis [*Ishida et al.*, 1996; *Kenzo et al.*, 2003]. Fully expanded and apparently nonsenescing leaves were sampled. Leaf age was estimated on the basis of

Table 2. Tree Species Included in the Gas Exchange Property Measurements[a]

Species	n[b]	Height, m
Dryobalanops aromatica	7	2.5 (0.7)
Dryobalanops aromatica	4	46.6 (2.6)
Dipterocarpus glabosus	5	1.2 (0.3)
Dipterocarpus glabosus	3	13.1 (3.5)
Dipterocarpus glabosus	4	40.8 (2.3)
Shorea acuta	6	1.5 (0.2)
Shorea acuta	3	16.1 (2.2)
Shorea acuta	6	36.1 (2.1)
Shorea beccariana	6	1.5 (0.3)
Shorea beccariana	4	50.5 (1.5)
Shorea macroptera	6	2.0 (0.4)
Shorea macroptera	3	16.4 (1.6)
Shorea macroptera	3	25.1 (1.7)

[a]All species were measured at several heights. Numbers in parentheses indicate standard errors.
[b]Number of individuals sampled.

leaf color, the position on the branch and leaf texture [*Sobrado and Medina*, 1980; *Ishida et al.*, 1996]; leaf color was measured with a chlorophyll meter (SPAD-502, Konica Minolta Holdings, Tokyo, Japan). Gas exchange measurements were made using the third to fifth leaves from the top of the shoot, because these leaves had stable SPAD values [*Ishida et al.*, 1996].

[27] Following the gas exchange measurements, leaves were excised and their area and fresh mass were measured. After drying at 60°C for three days they were then weighted and nitrogen contents were determined with an NC analyzer (Sumigraph NC-900, Shimadzu, Kyoto, Japan).

3.5. Leaf Area Measurements

[28] Spatial variations in leaf area plus branches (plant area index; PAI) were measured in September 2002 using a pair of plant canopy analyzers (LAI-2000, Li-Cor, Lincoln, Nebraska). The horizontal variation in PAI was measured every 5 m in a 30 × 30 m^2 subplot (LA in Figure 1). Also, the vertical PAI profiles of were measured at 1-m intervals in the upper canopy or 5-m intervals in the lower canopy along four vertical observation lines using the gondola (D1–D4 in Figure 1); the total number of observation points was 57. In this study, leaf area index (LAI) is assumed to be PAI. From the PAI observation results, the horizontal variation in leaf area density profiles was estimated.

3.6. Flux Measurements

[29] A three-dimensional sonic anemometer (DA-600, Kaijo, Tokyo, Japan) was installed at 60.2 m, i.e., 20 m above the mean canopy height, with an open-path CO_2/H_2O analyzer (LI-7500, Li-Cor, Lincoln, Nebraska) placed about 30 cm away. In addition, a ventilated psychrometer (MS020S, EKO, Tokyo, Japan) installed adjacent to the sonic anemometer and open path analyzer was used for calibration and correction of the density effects [*Webb et al.*, 1980]. Wind speeds and gas concentration time series were all sampled at 10 Hz. All variances and covariances required for the eddy covariance flux estimates were computed over a 30-min averaging interval. CO_2 concentration profile measurements within the canopy were carried out about 70 m from the crane. Air samples were obtained at 1.5, 6.5, 11.5, 21.5, 31.5 and 41.5 m above ground level using diaphragm pumps and an auto solenoid switching system, and CO_2 concentrations were measured using a closed path CO_2 infrared gas analyzer (LI-800, Li-Cor, Lincoln, Nebraska). The net ecosystem CO_2 exchange (NEE) was derived as the sum of the above-canopy CO_2 flux, which was obtained using the eddy covariance system above the canopy, and within-canopy storage flux, which was determined by quantifying the rate of change of the CO_2 concentration in the air column within the canopy. Canopy transpiration rates can be obtained as the above-canopy H_2O flux when the canopy is dry. Note that although soil evaporation is insignificant compared to the total transpiration flux (given the high LAI at the site) [e.g., *Kelliher et al.*, 1995], we took soil evaporation into consideration in our model (see (10)). Details on the eddy covariance measurements and estimation of NEE are presented by *Kumagai et al.* [2004c] and *Kumagai et al.* [2004a], respectively.

[30] The soil CO_2 efflux was measured manually in 2002 (DOY 134–137, 234–235, 306–308 and 341–343) using a portable IRGA (LI-6400, Li-Cor, Lincoln, Nebraska) connected to a chamber (6400-09 soil CO_2 flux chamber, Li-Cor, Lincoln, Nebraska) at 25 points every 10 m in a 40 × 40 m^2 subplot. Soil CO_2 efflux data were averaged over the subplot for each measurement day and regarded as the daytime average values of soil respiration rate. Since there were small variations in soil temperature (25°–28°C) at a depth of 2 cm during the measurement period, the dependency of daytime average soil respiration (R_{soil}) on temperature could not be discerned. Moreover, the relationship between R_{soil} and soil moisture was not significant. Thus daytime R_{soil} was regarded as a constant of 5.73 μmol m^{-2} s^{-1}, computed by averaging the daytime R_{soil}.

[31] Throughout the study period, using this constant value, the lower boundary condition for the scalar continuity and turbulent flux equations for CO_2 is given by:

$$m_a g_{Hs}\left[C_a(z_g) - C_a(z_g + \Delta z)\right] = 5.73 \tag{24}$$

Note that with a longer-period study, R_{soil} should not be constant mainly because of the effect of unpredictable intra-annual dry spells in this rain forest [*Kumagai et al.*, 2004c].

[32] We selected a study period spanning from DOY 247 (4 September) to 263 (20 September) in 2002 because of the availability of leaf-level physiological and leaf area density data synchronous with the flux measurements. Also, we only compared model outputs to the daytime (0600 to 1800 LT) NEE data because CO_2 fluxes during nighttime conditions were virtually all underestimated in the study site [*Saitoh et al.*, 2005].

4. Results and Discussion

[33] For practical implementation of the SVAT model for tropical forests, it is first necessary to examine how sensitive the flux calculations are to spatial variations in leaf-level physiological parameters and leaf area densities. In the following, we therefore discuss the observed spatial variations then test our SVAT model by conducting several numerical experiments that take these variations into considerations. Comparisons with the eddy-covariance-mea-

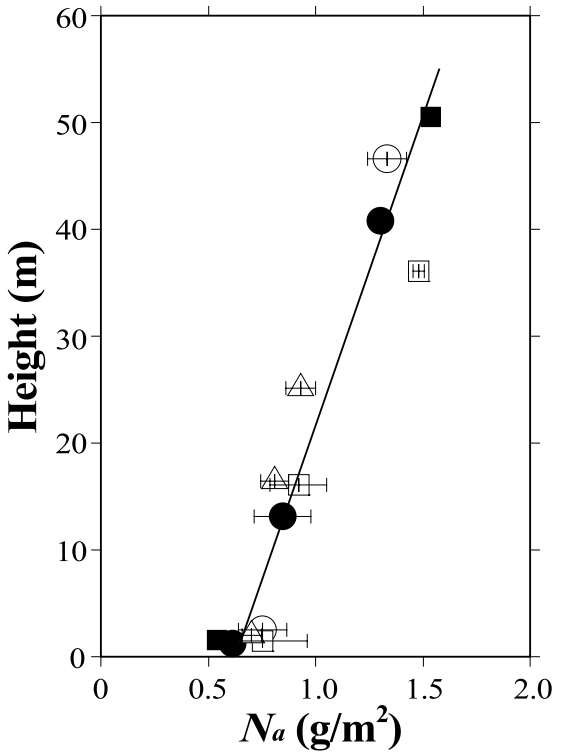

Figure 2. Relationship between leaf nitrogen per unit area (N_a) and canopy height (z). Horizontal bars represent one standard error. The regression equation is $N_a = 0.0173\ z + 0.627$ (solid line, $R^2 = 0.91$). Open circles indicate *Dryobalanops aromatica*, solid circles indicate *Dipterocarpus glabosus*, open squares indicate *Shorea acuta*, solid squares indicate *Shorea beccariana* and open triangles indicate *Shorea macroptera* (see Table 2).

sured CO_2 fluxes as well as a sensitivity analysis to the numerical experiments are also discussed.

4.1. Leaf-Level Physiological Parameters

[34] The vertical distribution of N_a within the canopy across all measured trees is shown in Figure 2. As shown by *Carswell et al.* [2000], foliar nitrogen concentration increased significantly with height (z) when expressed on a leaf area basis, but not when expressed on a total leaf mass basis [*Kenzo et al.*, 2004]. The average N_a was computed in each height class for each tree species (see Table 2) and the regression model describing z and bin-averaged N_a across all measured tree species was derived as follows: $N_a = 0.0173z + 0.627$, $R^2 = 0.91$. The N_a of individual leaves is generally correlated with the light environment, and as a result, its vertical distribution within the canopy is generally related to cumulative LAI profiles and the light attenuation coefficient [*Hirose and Werger*, 1987]. However, our approach assumes that the cumulative LAI profile is horizontally averaged. In this study, leaves for nitrogen content analysis were sampled vertically and horizontally within the canopy, thus the N_a profile was not one-dimensionally described as a function of the cumulative LAI, but rather, was determined as a function of z using a linear regression. By including the difference in species and horizontal variation in sample positions, this linear regression model clearly explained the vertical variation in N_a (Figure 2). *Dolman et al.* [1991] reported that the stomatal conductance and variation in conductance among trees at the same level in an Amazonian tropical rain forest canopy were similar. Similarly, the leaf-level physiological parameters were determined by height despite differences among species.

[35] Figure 3 shows $V_{cmax,25}$ as a function of N_a across species and measurement positions (see Table 2). Variability in $V_{cmax,25}$ as a result of species differences or positions within the canopy can be statistically explained by changes in N_a ($V_{cmax,25} = 28.01N_a + 3.41$, $R^2 = 0.62$). According to *Carswell et al.* [2000], Amazonian rain forest trees have a larger N_a than Bornean rain forest trees (1.5–4.5 versus 0.5–1.7 g m^{-2}). However, since the slope of the linear regression for Bornean rain forest trees was much higher, the $V_{cmax,25}$ in this study was more similar to those of Amazonian rain forest trees (10–60 μmol m^{-2} s^{-1}). Moreover, the relationship between N_a and $V_{cmax,25}$ in this study was comparable with that of the temperate deciduous forest reported by *Wilson et al.* [2000]. In addition, the R_F (see (20)) estimated in this study was 0.22, which is possibly much larger than that for Amazonian rain forest trees [*Carswell et al.*, 2000].

[36] Despite differences among species and canopy positions, $J_{max,25}$ was also explained by N_a thereby suggesting a strong correlation between $V_{cmax,25}$ and $J_{max,25}$ ($J_{max,25} = 2.52V_{cmax,25} - 12.54$, $R^2 = 0.88$) (Figure 4). Forcing the regression line through the origin decreased the estimated slope to 2.16 ($R^2 = 0.86$). *Wullschleger* [1993] showed a wide range of V_{cmax} and J_{max} values for 109 C_3 species, and despite multifold differences between species, revealed a strong correlation between V_{cmax} and J_{max}. Although our ranges for $J_{max,25}$ and $V_{cmax,25}$ were much smaller than

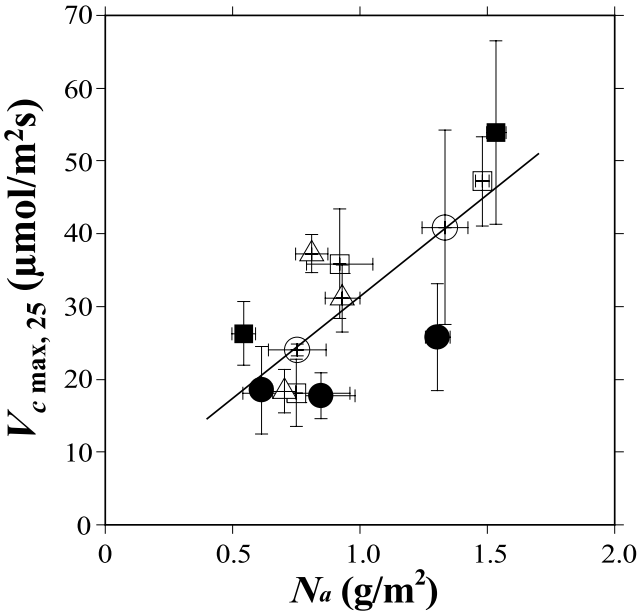

Figure 3. Relationship between leaf nitrogen per unit area (N_a) and the maximum Rubisco catalytic capacity at 25°C ($V_{cmax,25}$). Vertical and horizontal bars represent one standard error. The regression equation is $V_{cmax,25} = 28.01N_a + 3.41$ (solid line, $R^2 = 0.62$). Symbols are as in Figure 2.

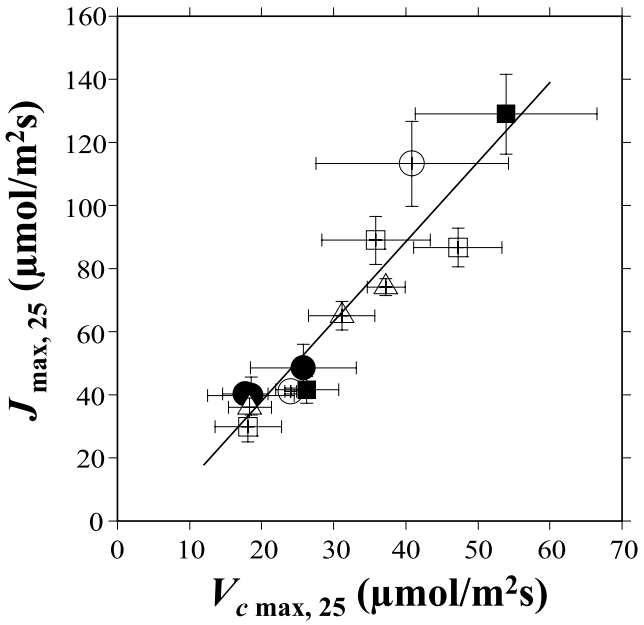

Figure 4. Relationship between the maximum Rubisco catalytic capacity ($V_{cmax,25}$) and maximum rate of electron transport ($J_{max,25}$) at 25°C. Vertical and horizontal bars represent one standard error. The regression equation is $J_{max,25} = 2.52V_{cmax,25} - 12.54$ (solid line, $R^2 = 0.88$). Symbols are as in Figure 2.

those of *Wullschleger* [1993], the ratio between them (i.e., $J_{max,25}/V_{cmax,25}$) was similar.

[37] No clear relationships were obtained between m and b (see (18)) and species or canopy positions; therefore constant values of m and b close to the means determined from the measurements (5.0 and 0.03, respectively) were assumed across species and throughout the canopy. Errors due to this assumption were thought to be minimal because any inaccuracies in the b estimations in this study had little impact on the canopy flux calculations and, except for trees close to the forest floor, variations in the determined m were sufficiently small (m and b were measured as 4.9 ± 1.1 (standard deviation) and 0.04 ± 0.02, respectively, using trees over 10 m in height). *Baldocchi and Meyers* [1998] pointed out the accumulating body of evidence showing that m is a constrained parameter centering around 10 ± 20%; our m value for Bornean tropical rain forest trees was much lower than this. Note that although the Ball-Berry model (equation (18)) is widely used for describing stomatal conductance, little data on its applicability with leaf-level parameters have been published for tropical forests.

[38] The above information suggests that variation in leaf-level physiological parameters within the canopy can be largely described as a function of height, and that species and horizontal variations are likely to be less important for flux calculations in the SVAT model.

4.2. Leaf Area Densities and Flow Statistics

[39] Measurements of horizontal variation in LAI in the LA subplot (see Figure 1) revealed values ranging from 4.8 to 6.8 $m^2\ m^{-2}$ with a mean of 6.2 $m^2\ m^{-2}$. On the other hand, the cumulative LAI data measured downward from the top of the canopy from 57 observation points along four vertical observation lines (D1–D4, see Figure 1) showed a strong linear relationship between z and the cumulative LAI ($R^2 = 0.82$). A straight line representing this linear relationship, connecting two points (z, cumulative LAI) = (0, LAI) and (h, 0), can be generated from integration of constant vertical distributions of leaf area density. Hence we assumed that in this site, LAI varies horizontally between 4.8 and 6.8 $m^2\ m^{-2}$, and that at each horizontal position the value of leaf area density is vertically constant from the canopy top to the forest floor.

[40] Since when describing the variation in leaf-level physiological parameters we have only to present the one-dimensional vertical variation, how the flux calculations respond to changes in vertical distributions of leaf area density should also be examined. Thus we conducted four numerical experiments considering the results of leaf area density. In case 1, a LAI of 6.2 $m^2\ m^{-2}$, the mean observed LAI, with a constant leaf area density of 0.123 $m^2\ m^{-3}$ from the canopy top to forest floor was used in the SVAT model. Cases 2 and 3 assumed LAIs of 6.8 and 4.8 $m^2\ m^{-2}$, the upper and lower values of the observed LAI, with constant leaf area densities of 0.136 and 0.096 $m^2\ m^{-3}$, respectively. In most SVAT models, the leaf area density distribution is arbitrarily determined as one vertical profile because a tower is generally used to obtain measurements [e.g., *Lai et al.*, 2000a, 2000b; *Park and Hattori*, 2004]. To examine the effect of arbitrarily determined vertical distributions of leaf area density on flux calculations, we also constructed case 4 assuming a vertical distribution of leaf area density determined by one vertical observation line (see Figure 1), the LAI of which was 4.8 $m^2\ m^{-2}$.

[41] Figure 5 illustrates how each of the above numerical experiments modifies the velocity statistics profiles inside the canopy predicted by the second-order closure model [*Wilson and Shaw*, 1977]. To investigate the impact of variation in leaf area density profiles on the velocity statistics inside the canopy, we compared mean longitudinal wind velocities ($\overline{u}$) and standard deviations of vertical velocity (σ_w), which are critical in calculating the boundary layer conductances in (13)–(15) and the turbulent flux equation, respectively, in cases 1–4. In this comparison, velocity scales were normalized by the friction velocity u_*. From Figure 5, it is clear that $\overline{u}$ did not appreciably vary among cases 1–3, while σ_w significantly increased in case 3. Moreover, although $\overline{u}$ and σ_w in cases 1 and 2 were similar, the differences in $\overline{u}$ and σ_w between cases 3 and 4 were relatively large, despite the same LAI value (4.8 $m^2\ m^{-2}$).

4.3. Impact of Leaf Area Density Distribution Within the Canopy on Flux Calculations

[42] Steady state conditions were assumed for all flux calculations. With this assumption, for example, the calculated above-canopy CO_2 flux, F_c, can be compared with the measured NEE. Figure 6 shows the time series of net radiation, sensible heat flux, latent heat flux and CO_2 flux in case 1 compared with daytime (0600 to 1800 LT) measurements obtained from DOY 247 to 263, 2002. Our SVAT model clearly reproduced all time series, showing its ability to synthesize canopy transport of energy, water vapor and CO_2.

[43] Table 3 presents the statistical parameters of the comparisons between modeled and measured F_c for cases

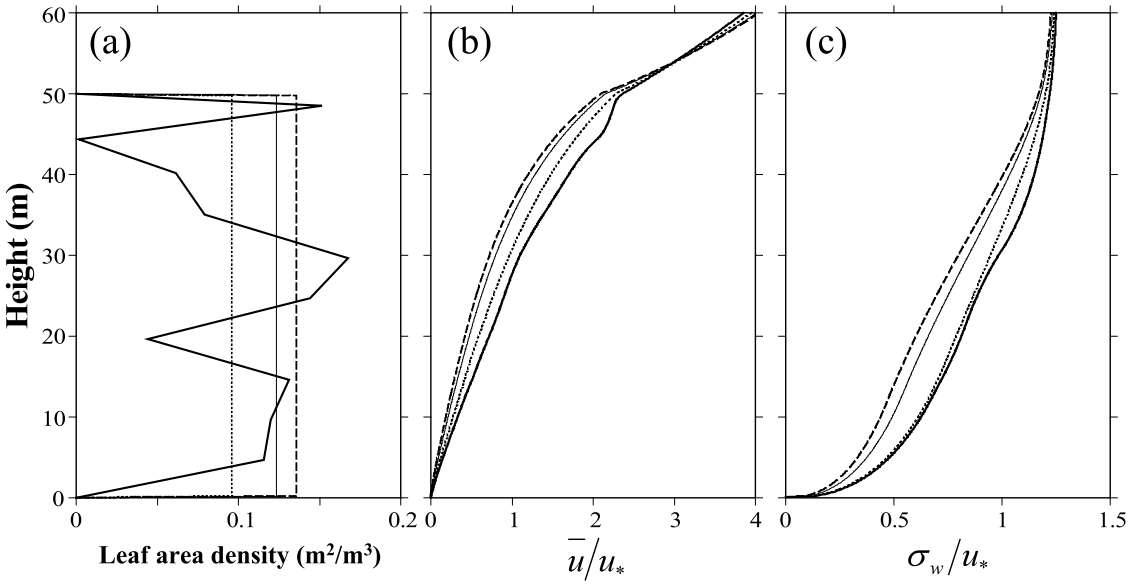

Figure 5. Vertical distributions of (a) plant area density, (b) modeled mean longitudinal wind velocities ($\overline{u}$) and (c) standard deviations of vertical velocity (σ_w) normalized by the friction velocity above the canopy (u_*) for cases 1 (thin solid line), 2 (dashed line), 3 (dotted line), and 4 (bold solid line).

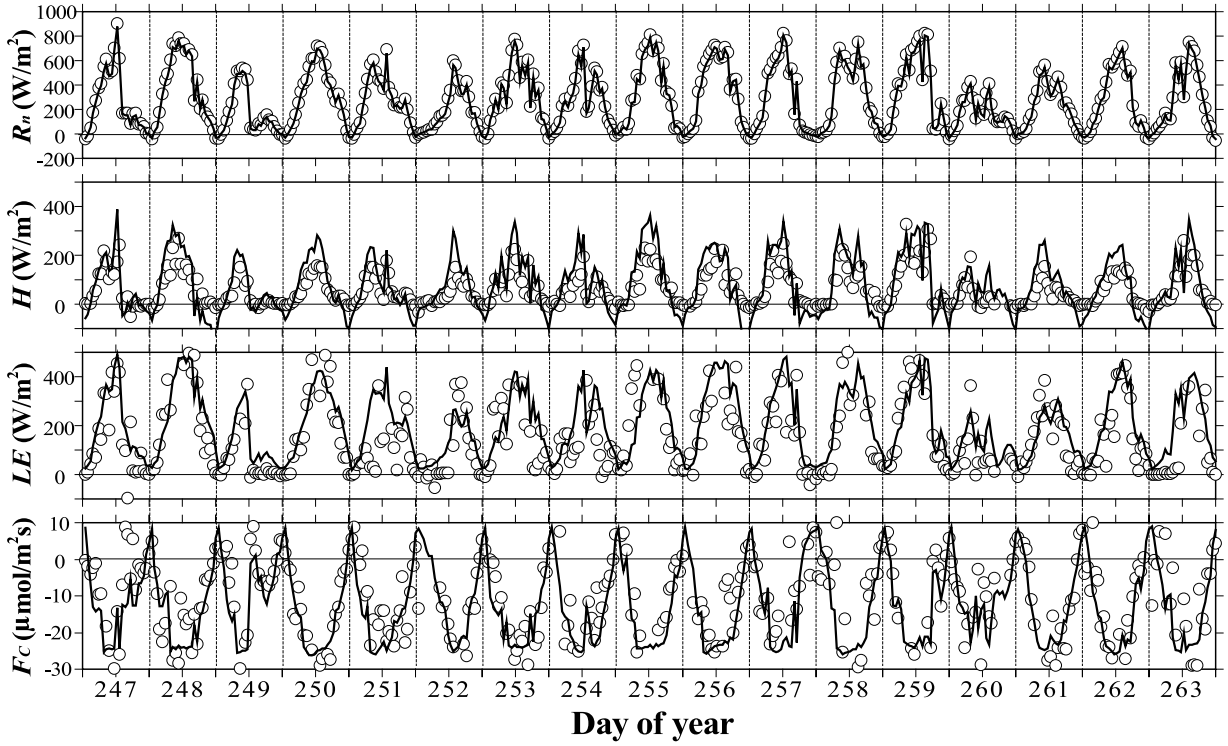

Figure 6. Measured (circles) time series of 30-min net radiation (R_n), sensible heat flux (H), latent heat flux (LE) and CO_2 flux (F_c) from DOY 247 (4 September) to 263 (20 September), 2002, and results modeled from case 1 (lines). The measured results represent daytime (0600 to 1800 LT) data.

Table 3. Regression Statistics for Comparisons Between the Measured and Modeled CO_2 Fluxes[a]

	Slope	Intercept, μmol m^{-2} s^{-1}	R^2	RMSE, μmol m^{-2} s^{-1}
Case 1	0.79	−0.80	0.62	6.95
Case 2	0.78	−1.05	0.62	6.93
Case 3	0.83	−0.29	0.61	6.89
Case 4	0.85	−0.35	0.61	6.78

[a]The regression model is y = Slope x + Intercept, where y and x are the measured and modeled CO_2 fluxes, respectively. The coefficient of determination (R^2) and root-mean-squared error (RMSE: μmol m^{-2} s^{-1}) are shown. The number of points in the regression analysis for each case was 341.

1–4. It is clear that changes in the vertical distribution of leaf area density had little impact on the modeled F_c, despite changes in the velocity statistics (see Figure 5) and absorbed radiation at different levels within the canopy. Further comparisons between the measured and modeled F_c bin-averaged by time of day are shown in Figure 7. It should be noted that the modeled F_c showed biases, i.e., overestimations (see also Table 3). In this study, the measured energy balance was not completely closed; the closure deficit was about 20%. That is, the energy balance relationship in this site most likely means that the eddy fluxes were underestimated by about 20% [*Kumagai et al.*, 2004c, 2005]. Thus the slopes of the regression model between the measured and modeled F_c (about 0.8, see Table 3) might be attributed to this underestimation of eddy fluxes. All cases recreated the canonical form of the measured F_c throughout all photosynthesis periods, implying that efforts to measure the detailed leaf area density distribution within the canopy do not always improve the predictive accuracy of the model. Reproducing both spatial and temporal patterns of the mean concentration field, a state variable influenced by combined source variation and turbulent transport mechanics, is one of the strengths of using a multilayer SVAT model [e.g., *Lai et al.*, 2000b]. However, while our model calculations of F_c clearly reproduced the measurements, those of the scalar profiles inside the canopy did not match the measured values. This implies that a simpler description of velocity statistics, in control of turbulent transport, like those proposed by *Raupach* [1989], *Baldocchi* [1992] and *Baldocchi and Meyers* [1998] might be sufficient.

[44] At different levels within the canopy, absorbed radiation altered by changes in the vertical distribution of leaf area density mainly drives changes in the physiological sources and sinks. Thus we proceeded to compare the CO_2 source strength distributions estimated with cases 1–4. Figure 8 shows the contour maps of these distributions as a function of time of day and height. In contrast to the calculated F_c, there were pronounced discrepancies between the estimated source strength distributions. In cases 1–3 (Figures 8a–8c, respectively), cases with a higher LAI had higher CO_2 uptake in the upper canopy layers but lower uptake in the lower canopy. In case 4 (Figure 8d), on the other hand, CO_2 uptake was high at heights of about 50 and 30 m where leaf area densities are also high.

[45] To assess how the CO_2 source strength distribution is formed, we conducted a study on the competition between J_E and J_C (see (19)) throughout the canopy, which is the limiting factor for A_l at each canopy level. Figure 9 shows the vertical profiles of CO_2 source strengths estimated from only J_E or J_C (hereinafter referred to as S_{JE} and S_{JC} (μmol m^{-3} s^{-1}), respectively) and averaged around noon (1100–1300 LT). Here, taking into consideration J_E and J_C for shaded and sunlit leaves, S_{JE} and S_{JC} were computed as J_{Esh} a_{sh} + J_{Esl} a_{sl} and J_{Csh} a_{sh} + J_{Csl} a_{sl} (where the subscripts *sl* and *sh* denote sunlit and shaded leaves), respectively. It should be noted that the minimum of J_E and J_C determines A_l. In the upper canopy layers, owing to the abundance of

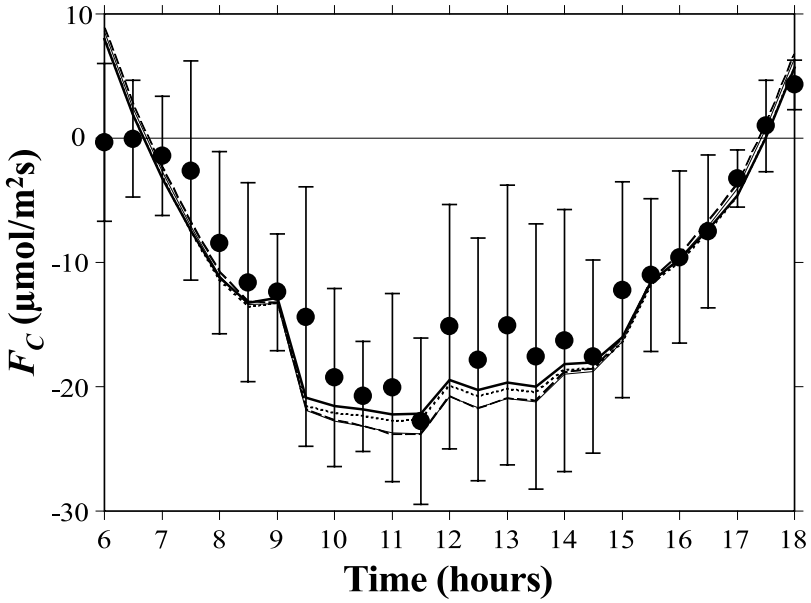

Figure 7. Average temporal variation in measured (solid circles) CO_2 fluxes (F_c) and results modeled from cases 1 (thin solid line), 2 (dashed line), 3 (dotted line), and 4 (thick solid line). For reference, one standard deviation of the measured binned F_c is also shown.

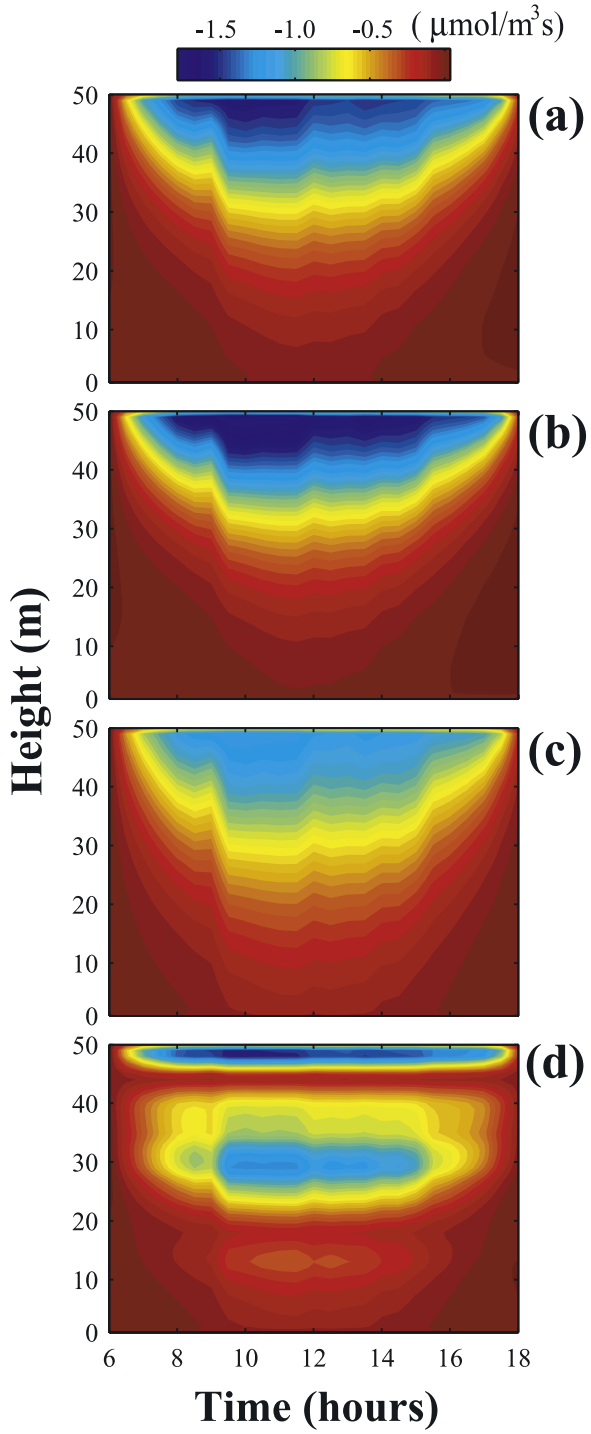

Figure 8. Contour plots of the average CO_2 source/sink distributions within the canopy as a function of height and time of day for cases (a) 1, (b) 2, (c) 3, and (d) 4.

light, S_{JC} was less than S_{JE} and determined the CO_2 uptake. With a higher LAI, S_{JC} was equal to S_{JE} at a higher position, because cases with a higher LAI had a more significant reduction in S_{JC} and S_{JE} in the upper canopy (Figures 9a–9c). In case 4, S_{JC} was equal to S_{JE} at a relatively lower position (35 m height), but S_{JC} was similar to S_{JE} in the upper canopy (Figure 9d). In the lower canopy, S_{JE} was less than S_{JC} because of attenuated light, and determined the CO_2 uptake. In cases with a lower LAI, light attenuation was small in the lower canopy, resulting in a small reduction in S_{JE} (Figures 9a–9c). Thus, in the upper canopy, the CO_2 uptake in case 3 was less than in cases 1 and 2, and vice versa in the lower canopy; for example, S_{JE} at 30 m in cases 1–3 were 0.49, 0.48 and 0.53 μmol m^{-3} s^{-1}, respectively.

[46] Figure 10 compares the profiles of average CO_2 flux without soil respiration (F_A) around noon (1100–1300 LT) modeled from cases 1–4, described as a function of the cumulative LAIs measured downward from the top of the canopy. Note that F_A denotes the CO_2 flux in each canopy layer expressed per unit area of ground. Therefore F_A at cumulative LAI = 0 is equal to the above-canopy F_c without soil respiration and decreases with increasing cumulative LAI. Moreover, it should also be noted that the cumulative LAI is not necessarily related to canopy height. In contrast to the source strength distributions, there were no large differences between flux profiles with each case. Figure 10 reveals that in cases 1 and 2, which have a high LAI, CO_2 uptake by leaves in the lower canopy layers contributed little to F_A because of the small S_{JE} in the lower canopy. Therefore, despite the different distributions of leaf area density, a greater part of the above-canopy F_c was generated by a constant cumulative LAI integrated from the canopy top of about 4.8 m^2 m^{-2}. Hence the above-canopy F_c appears robust to changes in leaf area density distributions, and with all cases the results were almost identical.

4.4. Impact of Nitrogen Distribution Within the Canopy on Flux Calculations

[47] Given the strong vertical gradients of leaf photosynthetic capacity in tropical forest canopies, it is instructive to investigate the impacts of these vertical gradients on F_c. This might be of use in framing a strategy for measuring leaf-level physiological parameters, because it is relatively difficult to gain access to some positions within the canopy.

[48] N_a is a key physiological parameter in our SVAT model. N_a averaged across species in height classes 0–5 (30 individuals) and 40–55 m (10 individuals) were 0.68 (±0.25 standard deviation) and 1.41 (±0.14) g m^{-2}, respectively. Using the vertical distribution of leaf area density in case 1, we constructed two further numerical experiments, cases 5A and 5B, which had constant vertical distributions of N_a (0.68 and 1.41 g m^{-2}, respectively). In other words, cases 5A and 5B assume that the N_a measured in the lower and upper canopies, respectively, is distributed evenly throughout, and evaluate the F_c variation caused by these two "end members" of vertical distribution assuming that the entire profile represents either the N_a in the lower or upper canopy. Figure 11 compares the F_c modeled from cases 1, 5A and 5B, bin-averaged by the time of day. While the F_c with case 5A was about half that with case 1, that with case 5B was almost the same as with case 1.

[49] Figure 12 compares the average vertical profiles of S_{JE} and S_{JC} around noon (1100–1300 LT) modeled from cases 1 and 5B. The heights where S_{JE} was equal to S_{JC} were almost the same with cases 1 and 5B. Despite large difference in S_{JC}, the vertical profiles of S_{JE} were similar. In summary, while the vertical distribution of N_a significantly altered the vertical profile of S_{JC}, that of S_{JE} was impacted less mainly because of light attenuation in the lower canopy.

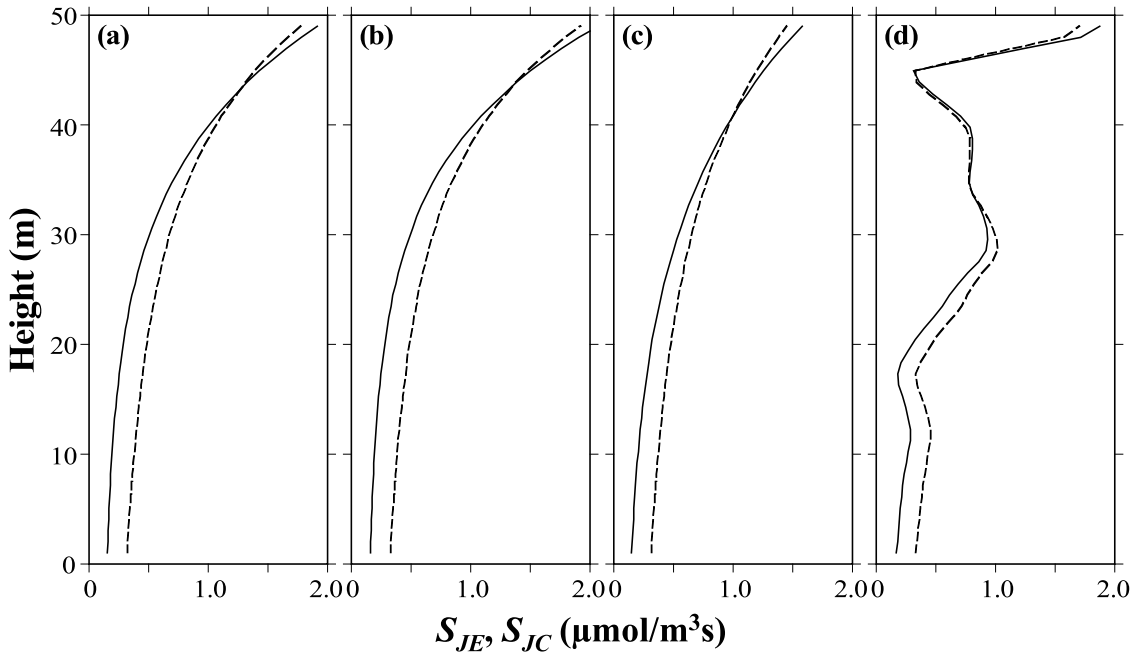

Figure 9. Average vertical profiles of CO_2 source strengths estimated from the gross rate of photosynthesis limited by the rate of ribulose bisphosphate (RuBP) regeneration through electron transport (S_{JE}, solid line) or RuBP carboxylase-oxygenase (Rubisco) activity (S_{JC}, dashed line) around noon (1100–1300 LT) modeled from cases (a) 1, (b) 2, (c) 3 and (d) 4.

As a result, the similarity in S_{JE}, which was the minimum of S_{JC} and S_{JE} and determined CO_2 uptake in most canopy layers, resulted in similar F_c in cases 1 and 5B (see Figure 11). This result also suggests that the N_a distributed within the canopy in case 5B was futile for the photosynthetic capacity of the lower canopy layers. Further comparisons of the canopy-level nitrogen use efficiency confirmed the apparently futile N_a in case 5B (-0.060 and -0.046 $\mu molCO_2\ m^{-2}s^{-1}\ mmolN^{-1}m^2$ in cases 1 and 5B, respectively). As has been pointed out previously [e.g., *Hirose and Werger*, 1987; *Sellers et al.*, 1992; *Kull and Jarvis*, 1995; *de Pury and Farquhar*, 1997], this also implies that a decrease in N_a with decreasing canopy height, as with the vertical distribution of N_a in case 1, might be the optimal distribution of limited nitrogen resources throughout the canopy that does not result in futile nitrogen resources and maximizes the photosynthetic carbon gain.

5. Conclusions

[50] Using a canopy crane, we were able to measure spatial variations in leaf-level physiological parameters and leaf area densities within the canopy of a Southeast Asian tropical rain forest. Considering the obtained results, we then compared the performance of SVAT, a multilayer biosphere-atmosphere model, with eddy covariance measurements. Since the SVAT model can reproduce detailed ecophysiological and turbulent transport processes within the canopy, from this combination of field measurements and analysis the following was demonstrated:

[51] 1. Despite differences in species and canopy positions, N_a within the canopy could be described as a linear function of height. Since N_a is the key physiological parameter in our SVAT model, which was shown to clearly

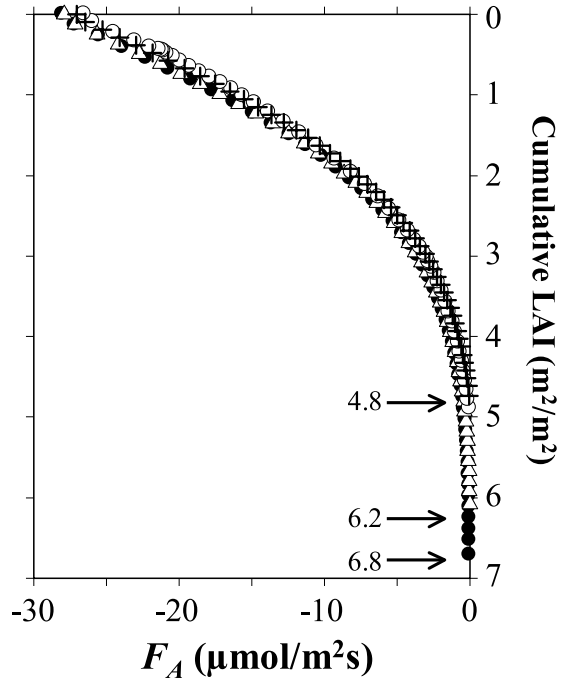

Figure 10. Vertical profiles of the average CO_2 flux without soil respiration (F_A) around noon (1100–1300 LT) as a function of cumulative leaf area index (LAI) modeled from cases 1 (open triangles), 2 (solid circles), 3 (crosses), and 4 (open circles). The LAI values (6.8, 6.2 and 4.8) are also shown.

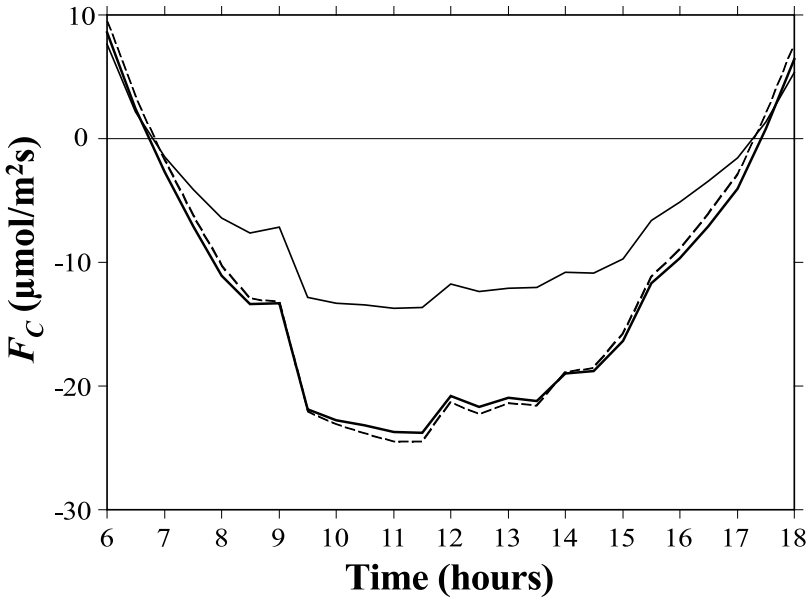

Figure 11. Average temporal variation in CO_2 fluxes (F_c) modeled from cases 1 (thick solid line), 5A (thin solid line), and 5B (dashed line). Cases 5A and 5B included constant vertical distributions of N_a (0.68 and 1.41 gm^{-2}, respectively).

explain $V_{c\max}$ and $J_{\max}$ across species and canopy positions, this implies that the leaf-level physiological parameter distributions are also linear functions of height that can be described one-dimensionally.

[52] 2. Using the above leaf-level physiological parameters and horizontally-averaged leaf area density profiles, our SVAT model reasonably reproduced the eddy covariance measurements. However, even when the leaf area density profile variations likely in this forest were used, the flux calculations varied little. This, in part, was attributed to the fact that increases in LAI increases CO_2 uptake in the upper canopy but decreases that in the lower canopy. Thus increased LAI (and hence increased radiation absorption in the upper canopy) was compensated for by reduced radiation in the lower canopy resulting in little overall change in F_c.

[53] 3. In reality, there was a strong vertical gradient of N_a in this tropical forest; however, the CO_2 source distribution calculated on the assumption that the N_a in the upper canopy was distributed evenly throughout, was almost the same as that taking the vertical gradient into consideration, resulting in little overall change in F_c. We found that light attenuation determines the source strength distribution, and that N_a distributed within the canopy is futile for the photosynthetic capacity in the lower canopy.

[54] These findings suggest that the SVAT model, which describes a forest canopy by the area-averaged representation, can be applied to this tropical rain forest, where considerable heterogeneities of canopy structure and leaf-level physiological properties are observed. Furthermore, to reproduce the above-canopy F_c, detailed information on leaf area density and leaf-level physiological property profiles were not significant; rather, the leaf area density profile obtained by evenly distributing the LAI measured at one-point and the leaf-level physiological parameters measured across species in the upper canopy were sufficient. The

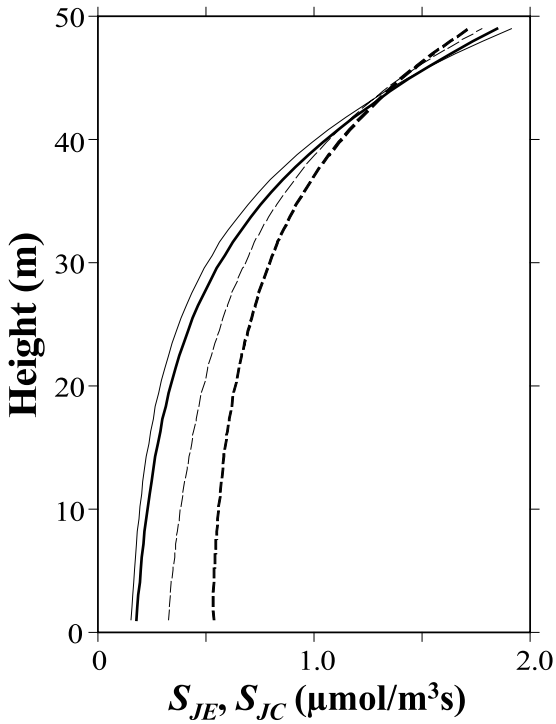

Figure 12. Average vertical profiles of CO_2 source strengths estimated from the gross rate of photosynthesis limited by the rate of ribulose bisphosphate (RuBP) regeneration through electron transport (S_{JE}) or RuBP carboxylase-oxygenase (Rubisco) activity (S_{JC}) around noon (1100–1300 LT). Thin and thick solid lines represent S_{JE} modeled from cases 1 and 5B, respectively, and thin and thick dashed lines represent S_{JC} modeled from cases 1 and 5B, respectively.

model results also imply that when the LAI is more than a certain value, the above-canopy F_c is conservative against LAI. The conclusions from this analytical study could allow a simple and straightforward treatment of tropical forest canopies, and are further attractive for the global climate and carbon balance models.

Appendix A: Radiative Transfer

[55] Radiative transfer through the canopy was modeled according to *Tanaka* [2002] with some modifications. A review and description of the radiative transfer process is provided below for completeness.

A1. Probability of No Contact With Direct or Diffuse Irradiance Within a Canopy

[56] The probability of no contact with direct irradiance within a canopy between z and $z + \Delta z$, P_b, is:

$$P_b = 1 - k_b a_{leaf} \Delta z \tag{A1}$$

where z is the height from the ground (m), k_b is the beam extinction coefficient, and a_{leaf} is the leaf area density within a given layer (m^2m^{-3}). Solar elevation β (radians) is geometrically calculated using the day of the year, the longitude and latitude of the site and the time of day. The beam extinction coefficient is a function of β and the leaf angle distribution within that layer and is defined by $k_b = G_{layer}/\sin\beta$ [*Goudriaan*, 1977], where G_{layer} is the ratio of the total leaf area within that layer in situ projected onto a plane normal to the direction β to $a_{leaf}\Delta z$. If the orientation angles of leaves within a layer are randomly distributed, G_{layer} can be obtained as follows:

$$G_{layer} = \int_0^{\pi/2} g_l(\alpha) \int_0^{2\pi} \frac{1}{2\pi} |\cos\alpha \sin\beta + \sin\alpha \cos\gamma \cos\beta| d\gamma d\alpha \tag{A2}$$

where α is the leaf inclination angle, γ is the leaf orientation angle, and $g_l(\alpha)$ is the inclination density function, expressed using the ratio of vertical to horizontal projections of canopy elements [*Campbell*, 1990].

[57] As diffuse irradiance is assumed to be isotropic, the probability of no contact within a canopy between z and $z + \Delta z$, P_d, is calculated by integrating P_b over the solid angles of the sky hemisphere with β as the angle of incidence of irradiance:

$$P_d = 2 \int_0^{\pi/2} P_b \sin\beta \cos\beta d\beta. \tag{A3}$$

A2. Direct and Diffuse Irradiances Within a Canopy

[58] The direct irradiance within a canopy is given by:

$$S_b(z) = P_b S_b(z + \Delta z) \tag{A4}$$

where S_b(z) is the direct PAR or NIR (Wm^{-2}) at height z. The downward and upward diffuse irradiances within a canopy are derived from the processes of transmission and reflectance of direct and diffuse irradiance by leaves, and are given by:

$$S_d^{\downarrow}(z) = [\eta(1 - P_d) + P_d] S_d^{\downarrow}(z + \Delta z) + \xi(1 - P_d) S_d^{\uparrow}(z) + \eta(1 - P_b) S_b(z + \Delta z) \tag{A5}$$

$$S_d^{\uparrow}(z + \Delta z) = [\eta(1 - P_d) + P_d] S_d^{\uparrow}(z) + \xi(1 - P_d) S_d^{\downarrow}(z + \Delta z) + \xi(1 - P_b) S_b(z + \Delta z) \tag{A6}$$

where S_d(z) is the diffuse PAR or NIR (Wm^{-2}) at height z. The superscript arrows denote the directions of irradiance, and η and ξ are the leaf transmissivity and reflectivity, respectively, for PAR or NIR. The irradiance reflected by the soil surface is expressed as:

$$S_d^{\uparrow}(0) = \xi_s \left[S_b(0) + S_d^{\downarrow}(0) \right] \tag{A7}$$

where ξ_s is the soil reflectivity for PAR or NIR.

A3. Determination of the Sunlit and Shaded Leaf Area Densities

[59] Using the direct PAR or NIR calculated by (A4), the sunlit and shaded leaf area densities (a_{sl} and a_{sh}, respectively; m^2m^{-3}) between z and $z + \Delta z$ are given by:

$$a_{sl} = \frac{[S_b(z + \Delta z) - S_b(z)] \sin\beta}{S_{b0} \Delta z G_{layer}} \tag{A8}$$

$$a_{sh} = a_{leaf} - a_{sl} \tag{A9}$$

where S_{b0} is the direct PAR or NIR over the canopy (Wm^{-2}).

A4. Thermal Radiation Within a Canopy

[60] Using the leaf temperature, T_c (K), and theory for diffuse irradiance transfer within a canopy between z and $z + \Delta z$, the downward and upward thermal radiations, L, are given by:

$$L^{\downarrow}(z) = P_d L^{\downarrow}(z + \Delta z) + (1 - P_d) \varepsilon_l \sigma \left(a_{sl} T_{csl}^4 + a_{sh} T_{csh}^4 \right) / a_{leaf} \tag{A10}$$

$$L^{\uparrow}(z + \Delta z) = P_d L^{\uparrow}(z) + (1 - P_d) \varepsilon_l \sigma \left(a_{sl} T_{csl}^4 + a_{sh} T_{csh}^4 \right) / a_{leaf}, \tag{A11}$$

where ε_l is the leaf emissivity and σ is the Stefan-Boltzmann constant (5.67×10^{-8} $Wm^{-2}K^{-4}$). The subscripts *sl* and *sh* denote sunlit and shaded leaves, respectively.

[61] **Acknowledgments.** We are grateful to the Forestry Department, Sarawak, for their support during this study. We also thank Tohru Nakashizuka for his support and the numerous colleagues who helped us with this work. This work was funded by CREST (Core Research for Evolutional Science and Technology) of JST (the Japan Science and Technology Agency) and a grant from the Ministry of Education, Science and Culture, Japan (16310017).

References

Badger, M. R., and G. J. Collatz (1977), Studies on the kinetic mechanism of ribulose-1,5–bisphosphate carboxlase and oxygenase reactions, with particular reference to the effect of temperature on kinetic parameters, *Year Book Carnegie Inst. Washington*, *76*, 355–361.

Baldocchi, D. (1992), A Lagrangian random-walk model for simulating water vapor, CO_2 and sensible heat flux densities and scalar profiles over and within a soybean canopy, *Boundary Layer Meteorol.*, *61*, 113–144.

Baldocchi, D., and T. Meyers (1998), On using eco-physiological, micrometeorological and biogeochemical theory to evaluate carbon dioxide, water vapor and trace gas fluxes over vegetation: A perspective, *Agric. For. Meteorol.*, *90*, 1–25.

Baldocchi, D. D., and K. B. Wilson (2001), Modeling CO_2 and water vapor exchange of a temperate broadleaved forest across hourly to decadal time scales, *Ecol. Model.*, *142*, 155–184.

Ball, J. T., I. E. Woodrow, and J. A. Berry (1987), A model predicting stomatal conductance and its contribution to the control of photosynthesis under different environmental conditions, in *Progress in Photosynthesis Research*, edited by J. Biggens, pp. 221–224, Springer, New York.

Cabral, O. M. R., A.-L. C. McWilliam, and J. M. Roberts (1996), Incanopy microclimate of Amazonian forest and estimates of transpiration, in *Amazonian Deforestation and Climate*, edited by J. H. C. Gash et al., pp. 207–219, John Wiley, Hoboken, N. J.

Campbell, G. S. (1990), Derivation of an angle density function for canopies with ellipsoidal inclination angle distribution, *Agric. For. Meteorol.*, *49*, 173–176.

Campbell, G. S., and J. M. Norman (1998), *An Introduction to Environmental Biophysics*, 2nd ed., Springer, New York.

Carswell, F. E., P. Meir, E. V. Wandelli, L. C. M. Bonates, B. Kruijt, E. M. Barbosa, A. D. Nobre, J. Grace, and P. G. Jarvis (2000), Photosynthetic capacity in a central Amazonian rain forest, *Tree Physiol.*, *20*, 179–186.

Collatz, G. J., J. T. Ball, C. Grivet, and J. A. Berry (1991), Regulation of stomatal conductance and transpiration: A physiological model of canopy processes, *Agric. For. Meteorol.*, *54*, 107–136.

de Pury, D. G. G., and G. D. Farquhar (1997), Simple scaling of photosynthesis from leaves to canopies without the errors of big-leaf models, *Plant Cell Environ.*, *20*, 537–557.

Dolman, A. J., J. H. C. Gash, J. Roberts, and W. J. Shuttleworth (1991), Stomatal and surface conductance of tropical rainforest, *Agric. For. Meteorol.*, *54*, 303–318.

Fan, S. M., S. C. Wofsy, P. S. Bakwin, and D. J. Jacob (1990), Atmosphere-biosphere exchange of CO_2 and O_3 in the central Amazon forest, *J. Geophys. Res.*, *95*(D10), 16,851–16,864.

Farquhar, G. D., and S. C. Wong (1984), An empirical model of stomatal conductance, *Aust. J. Plant Physiol.*, *11*, 191–210.

Farquhar, G. D., S. von Caemmerer, and J. A. Berry (1980), A biochemical model of photosynthetic CO_2 assimilation in leaves of C_3 species, *Planta*, *149*, 78–90.

Food and Agriculture Organization (1993), *Forest Resources Assessment 1990—Tropical Countries*, *FAO For. Pap. 112*, Rome.

Goudriaan, J. (1977), *Crop Micrometeorology: A Simulation Study*, Cent. for Agric. Publ. and Doc., Wageningen, Netherlands.

Grace, J., et al. (1995), Carbon dioxide uptake by an undisturbed tropical rain forest in southwest Amazonia, 1992 to 1993, *Science*, *270*, 778–780.

Grace, J., Y. Malhi, J. Lloyd, J. McIntyre, A. C. Miranda, P. Meir, and H. S. Miranda (1996), The use of eddy covariance to infer the net carbon dioxide uptake of Brazilian rain forest, *Global Change Biol.*, *2*, 209–217.

Grace, J., Y. Malhi, N. Higuchi, and P. Meir (2001), Productivity of tropical forests, in *Terrestrial Global Productivity*, edited by J. Roy et al., pp. 401–426, Elsevier, New York.

Hirose, T., and M. J. A. Werger (1987), Maximising daily canopy photosynthesis with respect to the leaf nitrogen allocation pattern in the canopy, *Oecologia*, *72*, 520–526.

Houghton, R. A., and J. L. Hackler (1999), Emissions of carbon from forestry and land-use change in tropical Asia, *Global Change Biol.*, *5*, 481–492.

Ishida, A., T. Toma, Y. Matsumoto, S.-K. Yap, and Y. Maruyama (1996), Diurnal changes in leaf gas exchange characteristics in the uppermost canopy of a rain forest tree, *Dryobalanops aromatica* Gaertn. f., *Tree Physiol.*, *24*, 1187–1192.

Ishida, A., T. Nakano, A. Umemura, N. Yamashita, H. Tanabe, and N. Koike (2001), Light-use properties in two sun-adapted shrubs with contrasting canopy structures, *Tree Physiol.*, *21*, 497–504.

Katul, G. G., and J. D. Albertson (1998), An investigation of higher-order closure models for a forested canopy, *Boundary Layer Meteorol.*, *89*, 47–74.

Katul, G. G., and J. D. Albertson (1999), Modeling CO_2 sources, sinks, and fluxes within a forest canopy, *J. Geophys. Res.*, *104*(D6), 6081–6091.

Kelliher, F. M., R. Leuning, M. R. Raupach, and E.-D. Schulze (1995), Maximum conductances for evaporation from global vegetation types, *Agric. For. Meteorol.*, *73*, 1–16.

Kenzo, T., T. Ichie, I. Ninomiya, and T. Koike (2003), Photosynthetic activity in seed wings of Dipterocarpaceae in a masting year: Does wing photosynthesis contribute to reproduction?, *Photosynthetica*, *41*, 551–557.

Kenzo, T., T. Ichie, R. Yoneda, Y. Kitahashi, Y. Watanabe, I. Ninomiya, and T. Koike (2004), Interspecific variation of photosynthesis and leaf characteristics in canopy trees of five species of Dipterocarpaceae in a tropical rain forest, *Tree Physiol.*, *24*, 1187–1192.

Koike, F. (1993), Canopy structure of a tropical rain forest and the nature of an unstratified upper layer, *Funct. Ecol.*, *7*, 230–235.

Kull, O., and P. G. Jarvis (1995), The role of nitrogen in a simple scheme to scale up photosynthesis from leaf to canopy, *Plant Cell Environ.*, *18*, 1174–1182.

Kumagai, T., K. Kuraji, H. Noguchi, Y. Tanaka, K. Tanaka, and M. Suzuki (2001), Vertical profiles of environmental factors within tropical rainforest, Lambir Hills National Park, Sarawak, Malaysia, *J. For. Res.*, *6*, 257–264.

Kumagai, T., G. G. Katul, A. Porporato, T. M. Saitoh, M. Ohashi, T. Ichie, and M. Suzuki (2004a), Carbon and water cycling in a Bornean tropical rainforest under current and future climate scenarios, *Adv. Water Res.*, *27*, 1135–1150.

Kumagai, T., G. G. Katul, T. M. Saitoh, Y. Sato, O. J. Manfroi, T. Morooka, T. Ichie, K. Kuraji, M. Suzuki, and A. Porporato (2004b), Water cycling in a Bornean tropical rain forest under current and projected precipitation scenarios, *Water Resour. Res.*, *40*, W01104, doi:10.1029/2003WR002226.

Kumagai, T., T. M. Saitoh, Y. Sato, T. Morooka, O. J. Manfroi, K. Kuraji, and M. Suzuki (2004c), Transpiration, canopy conductance and the decoupling coefficient of a lowland mixed dipterocarp forest in Sarawak, Borneo: Dry spell effects, *J. Hydrol.*, *287*, 237–251.

Kumagai, T., T. M. Saitoh, Y. Sato, H. Takahashi, O. J. Manfroi, T. Morooka, K. Kuraji, M. Suzuki, T. Yasunari, and H. Komatsu (2005), Annual water balance and seasonality of evapotranspiration in a Bornean tropical rainforest, *Agric. For. Meteorol.*, *128*, 81–92.

Lai, C.-T., G. Katul, D. Ellsworth, and R. Oren (2000a), Modelling vegetation-atmosphere CO_2 exchange by a coupled Eulerian-Lagrangian approach, *Boundary Layer Meteorol.*, *95*, 91–122.

Lai, C.-T., G. Katul, R. Oren, D. Ellsworth, and K. Schäfer (2000b), Modelling CO_2 and water vapor turbulent flux distributions within a forest canopy, *J. Geophys. Res.*, *105*(D21), 26,333–26,351.

Lai, C.-T., G. Katul, J. Butnor, M. Siqueira, D. Ellsworth, C. Maier, K. Johnsen, S. McKeand, and R. Oren (2002), Modelling the limits on the response of net carbon exchange to fertilization in a south-eastern pine forest, *Plant Cell Environ.*, *25*, 1095–1119.

Leuning, R., F. M. Kelliher, D. G. G. de Pury, and E.-D. Schulze (1995), Leaf nitrogen, photosynthesis, conductance and transpiration: Scaling from leaves to canopies, *Plant Cell Environ.*, *18*, 1183–1200.

Lloyd, J., J. Grace, A. C. Miranda, P. Meir, S. C. Wong, H. S. Miranda, I. R. Wright, J. H. C. Gash, and J. McIntyre (1995), A simple calibrated model of Amazon rainforest productivity based on leaf biochemical properties, *Plant Cell Environ.*, *18*, 1129–1145.

Malhi, Y., and J. Grace (2000), Tropical forests and atmospheric carbon dioxide, *Trends Ecol. Evol.*, *15*, 332–337.

Malhi, Y., A. D. Nobre, J. Grace, B. Kruijt, M. G. P. Pereira, A. Culf, and S. Scott (1998), Carbon dioxide transfer over a Central Amazonian rain forest, *J. Geophys. Res.*, *103*(D24), 31,593–31,612.

McWilliam, A.-L. C., O. M. R. Cabral, B. M. Gomes, J. L. Esteves, and J. M. Roberts (1996), Forest and pasture leaf-gas exchange in south-west Amazonia, in *Amazonian Deforestation and Climate*, edited by J. H. C. Gash et al., pp. 265–285, John Wiley, Hoboken, N. J.

Mellor, G. (1973), Analytic prediction of the properties of stratified planetary boundary layer, *J. Atmos. Sci.*, *30*, 1061–1069.

Nakashizuka, T., H. S. Lee, and L. Chong (2001), Studies on canopy processes of a tropical rain forest in Lambir Hills National Park, in *Proceedings of the International Symposium. Canopy Process and Ecological Roles of Tropical Rain Forest*, edited by T. Ichioka et al., pp. 2–7, Miri, Malaysia.

Niinements, U., and J. D. Tenhunen (1997), A model separating leaf structural and physiological effects on carbon gain along light gradients for the shade-tolerant species *Acer sccharum*, *Plant Cell Environ.*, *20*, 845–866.

Ozanne, C. M. P., et al. (2003), Biodiversity meets the atmosphere: A global view of forest canopies, *Science*, *301*, 183–186.

Park, H., and S. Hattori (2004), Modeling scalar and heat sources, sinks, and fluxes within a forest canopy during and after rainfall events, *J. Geophys. Res.*, *109*, D14301, doi:10.1029/2003JD004360.

Raupach, M. R. (1989), Applying Lagrangian fluid mechanics to infer scalar source distributions from concentration profiles in plant canopies, *Agric. For. Meteorol.*, *47*, 85–108.

Roberts, J., O. M. R. Cabral, and L. d. F. Aguiar (1990), Stomatal and boundary-layer conductances in an Amazonian terra firme rainforest, *J. Appl. Ecol.*, *27*, 336–353.

Roberts, J., O. M. R. Cabral, G. Fisch, L. C. B. Molion, C. J. Moore, and W. J. Shuttleworth (1993), Transpiration from an Amazonian rainforest calculated from stomatal conductance measurements, *Agric. For. Meteorol.*, *65*, 175–196.

Saitoh, T. M., T. Kumagai, M. Ohashi, T. Morooka, and M. Suzuki (2005), Nighttime CO_2 flux over a Bornean tropical rainforest, *J. Jpn. Soc. Hydrol. Water Resour.*, *18*, 64–72.

Saleska, S. R., et al. (2003), Carbon in Amazon forests: Unexpected seasonal fluxes and disturbance-induced losses, *Science*, *302*, 1554–1557.

Sato, Y., T. Kumagai, T. M. Saitoh, and M. Suzuki (2004), Characteristics of soil temperature and soil heat flux within tropical rainforest, Lambir Hills National Park, Sarawak, Malaysia, *Bull. Inst. Trop. Agric., Kyushu Univ.*, *27*, 55–63.

Sellers, P. J., J. A. Berry, G. J. Collatz, C. B. Field, and F. G. Hall (1992), Canopy reflectance, photosynthesis and transpiration. III. A reanalysis using improved leaf models and new canopy integration scheme, *Remote Sens. Environ.*, *42*, 187–216.

Siqueira, M., G. Katul, and C.-T. Lai (2002), Quantifying net ecosystem exchange by multilevel ecophysiological and turbulent transport models, *Adv. Water Res.*, *25*, 1357–1366.

Sobrado, M. A., and E. Medina (1980), General morphology, anatomical structure, and nutrient content of sclerophyllous leaves of the 'Bana' vegetation of Amazonas, *Oecologia*, *45*, 341–345.

Tanaka, K. (2002), Multi-layer model of CO_2 exchange in a plant community coupled with the water budget of leaf surfaces, *Ecol. Model.*, *147*, 85–104.

Taylor, J. A., and J. Lloyd (1992), Sources and sinks of atmospheric CO_2, *Aust. J. Bot.*, *40*, 407–418.

von Caemmerer, S., and G. D. Farquhar (1981), Some relationships between the biochemistry of photosynthesis and the gas exchange of leaves, *Planta*, *153*, 376–387.

von Caemmerer, S., J. R. Evans, G. S. Hudson, and T. J. Andrews (1994), The kinetics of ribrose-1, 5–bisphosphate carboxylase/oxygenase in vivo inferred from measurements of photosynthesis in leaves of transgenic tabaco, *Planta*, *195*, 88–97.

Vourlitis, G. L., N. Priante Filho, H. M. S. Hayashi, S. J. d. Nogueira, F. T. Caseiro, and J. J. H. Campelo (2001), Seasonal variations in the net ecosystem CO_2 exchange of a mature Amazonian transitional tropical forest (cerradão), *Funct. Ecol.*, *15*, 388–395.

Wang, Y. P., and P. G. Jarvis (1990), Description and validation of an array model—MAESTRO, *Agric. For. Meteorol.*, *51*, 257–280.

Watanabe, T. (1993), The bulk transfer coefficients over a vegetated surface based on K-theory and 2nd-order closure model, *J. Meteorol. Soc. Jpn.*, *71*, 33–42.

Watanabe, T., M. Yokozawa, S. Emori, K. Takata, A. Sumida, and T. Hara (2004), Developing a multilayered integrated numerical model of surface physics-growing plants interaction (MINoSGI), *Global Change Biol.*, *9*, 1378–1400.

Webb, E. K., G. I. Pearman, and R. Leuning (1980), Correction of flux measurements for density effects due to heat and water vapour transfer, *Q. J. R. Meteorol. Soc.*, *106*, 85–100.

Whittaker, R. H., and G. E. Likens (1975), The biosphere and man, in *Primary Productivity of the Biosphere*, edited by R. H. Whittaker and G. E. Likens, pp. 305–328, Springer, New York.

Williams, M., Y. Malhi, A. D. Nobre, E. B. Rastetter, J. Grace, and M. G. P. Pereira (1998), Seasonal variation in net carbon exchange and evapotranspiration in a Brazillian rain forest: A modelling analysis, *Plant Cell Environ.*, *21*, 953–968.

Wilson, K. B., D. D. Baldocchi, and P. J. Hanson (2000), Spatial and seasonal variability of photosynthetic parameters and their relationship to leaf nitrogen in a deciduous forest, *Tree Physiol.*, *20*, 565–578.

Wilson, N. R., and R. H. Shaw (1977), A higher order closure model for canopy flow, *J. Appl. Meteorol.*, *16*, 1198–1205.

Wullschleger, S. D. (1993), Biochemical limitations to carbon assimilation in C_3 plants-A retrospective analysis of the A/C_i curves from 109 species, *J. Exp. Bot.*, *44*, 907–920.

Yamada, T. (1992), Three-dimensional numerical model of atmospheric turbulence, in *Simulations of Atmospheric Environment*, edited by O. Yokoyama, pp. 134–202, Hakua-Shobo, Tokyo.

Yamakura, T., M. Kanzaki, A. Itoh, T. Ohkubo, K. Ogino, E. O. K. Chai, H.-S. Lee, and P. S. Ashton (1995), Forest architecture of Lambir rain forest revealed by a large-scale research plot, in *Reports of New Program for Promotion of Basic Sciences. Studies of Global Environmental Changes with Special Reference to Asia and Pacific Regions*, vol. II-3, *Long Term Ecological Research of Tropical Rain Forest in Sarawak*, edited by H.-S. Lee et al., pp. 2–20, Ehime Univ., Matsuyama, Japan.

T. Ichie, Faculty of Agriculture, Kochi University, Nankoku 783-8502, Japan.

T. Kenzo, Forestry and Forest Products Research Institute, Tsukuba 305-8687, Japan.

T. Koike, Hokkaido University Forests, FSC, Sapporo, 060-0809, Japan.

H. Komatsu, Institute of Industrial Science, University of Tokyo, Tokyo 106-8558, Japan.

T. Kumagai, Shiiba Research Forest, Kyushu University, Shiiba-son, Miyazaki 883-0402, Japan. (kuma@forest.kyushu-u.ac.jp)

M. Ohashi, Joensuu Research Center, Finnish Forest Research Institute, FI-80101 Joensuu, Finland.

T. M. Saitoh, River Basin Research Center, Gifu University, Gifu 501-1193, Japan.

M. Suzuki, Graduate School of Agricultural and Life Sciences, University of Tokyo, 1-1-1 Yayoi, Bunkyo-ku, Tokyo 113-8657, Japan.

M. Yamashita, Survey College of Kinki, 1-5-9 Yata, Higashi-Sumiyashi, Osaka 546-0023, Japan.

M. Yoshimura, Research Institute for Humanity and Nature, Kyoto 603-8047, Japan.